iScience

CellPress
OPEN ACCESS

Article

Increasing neuronal glucose uptake attenuates brain aging and promotes life span under dietary restriction in *Drosophila*

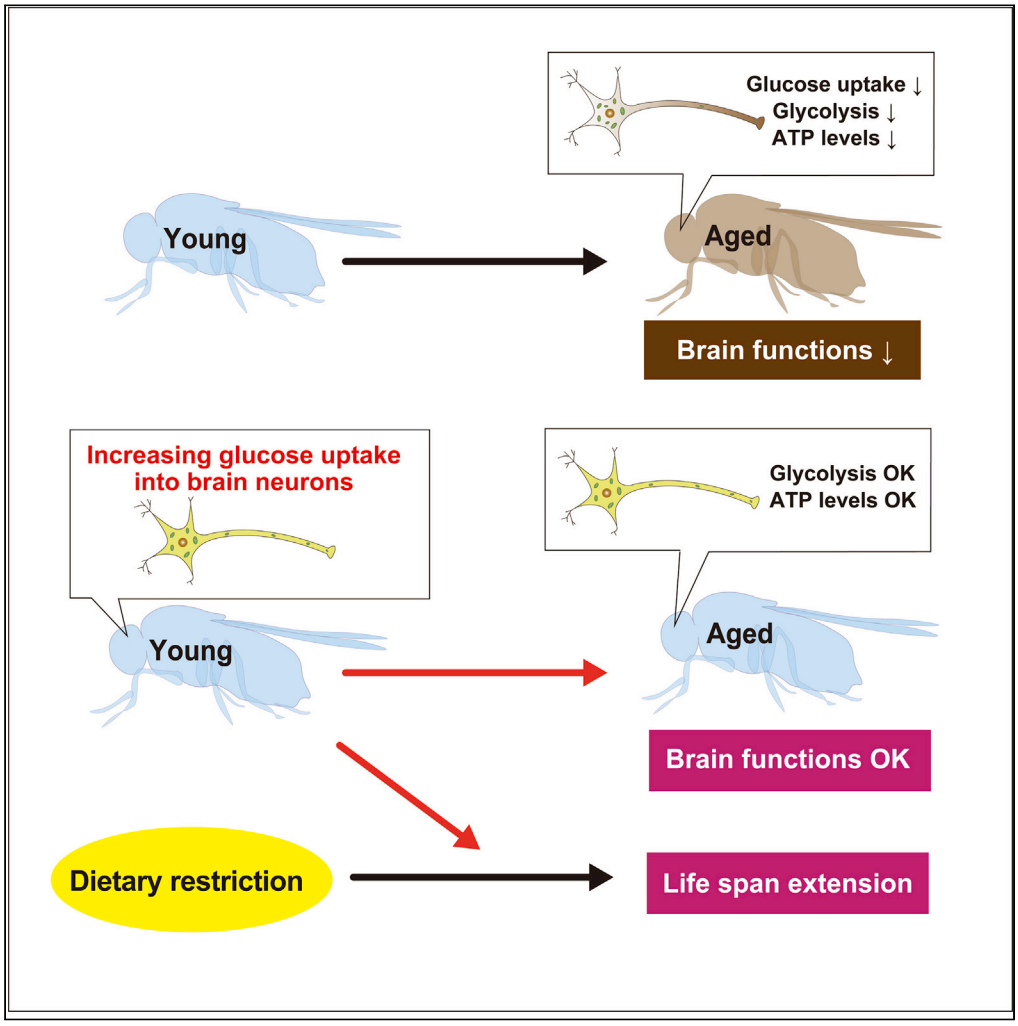

For a Figure360 author presentation of this figure, see https://doi.org/10.1016/j.isci.2020.101979

Mikiko Oka, Emiko Suzuki, Akiko Asada, Taro Saito, Koichi M. Iijima, Kanae Ando

k_ando@tmu.ac.jp

Highlights

Imaging of *Drosophila* brain reveals aged neurons suffer from energy deficits

Increased neuronal glucose uptake attenuates age-dependent declines in ATP

Increased glucose uptake is beneficial despite age-dependent mitochondrial damage

Increased neuronal glucose uptake and dietary restriction further extend life span

Oka et al., iScience *24*, 101979
January 22, 2021
https://doi.org/10.1016/j.isci.2020.101979

iScience

CellPress
OPEN ACCESS

Article

Increasing neuronal glucose uptake attenuates brain aging and promotes life span under dietary restriction in *Drosophila*

Mikiko Oka,[1] Emiko Suzuki,[1,3,4] Akiko Asada,[1,2] Taro Saito,[1,2] Koichi M. Iijima,[5,6] and Kanae Ando[1,2,7,*]

SUMMARY

Brain neurons play a central role in organismal aging, but there is conflicting evidence about the role of neuronal glucose availability because glucose uptake and metabolism are associated with both aging and extended life span. Here, we analyzed metabolic changes in the brain neurons of *Drosophila* during aging. Using a genetically encoded fluorescent adenosine triphosphate (ATP) biosensor, we found decreased ATP concentration in the neuronal somata of aged flies, correlated with decreased glucose content, expression of glucose transporter and glycolytic enzymes and mitochondrial quality. The age-associated reduction in ATP concentration did not occur in brain neurons with suppressed glycolysis or enhanced glucose uptake, suggesting these pathways contribute to ATP reductions. Despite age-associated mitochondrial damage, increasing glucose uptake maintained ATP levels, suppressed locomotor deficits, and extended the life span. Increasing neuronal glucose uptake during dietary restriction resulted in the longest life spans, suggesting an additive effect of enhancing glucose availability during a bioenergetic challenge on aging.

INTRODUCTION

Aging is associated with progressive declines in physiological integrity and functions alongside increases in vulnerability and the risk of developing a number of diseases (Kirkwood and Austad, 2000). The nervous system regulates motor and sensory functions and orchestrates metabolic control and stress responses in peripheral tissues *via* neuroendocrine signals (Alcedo and Kenyon, 2004; Burkewitz et al., 2015; Cohen et al., 2009; Libert et al., 2007; Satoh and Imai, 2014; Ulgherait et al., 2014; Zhang et al., 2018). Thus, age-associated changes in neurons are likely to play a critical role in organismal aging.

The brain requires a large amount of energy: it consumes about 20% of the oxygen and 25% of the glucose in the human body (Belanger et al., 2011; Mink et al., 1981; Raichle et al., 1970). Most of the adenosine triphosphate (ATP) required to support neuronal function is supplied by the metabolism of glucose through glycolysis and mitochondrial oxidative phosphorylation (Belanger et al., 2011). However, aging induces changes in both glucose availability and energy production, including declines in glucose uptake, electron transport chain activity, and aerobic glycolysis in the brain (Goyal et al., 2017; Hoyer, 2000). This implies that strategies aimed at increasing glucose metabolism in neurons may protect against organismal aging.

By contrast, dietary restriction (DR) and a reduction in insulin signaling have been demonstrated to have anti-aging effects (Guarente, 2008). DR causes circulating glucose concentrations to fall (Guarente, 2008). Thus, the pro-aging effects of reductions in brain glucose metabolism and the anti-aging effects of reducing insulin-stimulated glucose uptake are apparently contradictory. To resolve this discrepancy, it is necessary to elucidate how aging affects glucose metabolism in brain neurons and how such age-related changes in neurons interact with the anti-aging effects of DR.

In the present study, we show that aged brain neurons suffer from ATP deficits. Using a genetically encoded fluorescent ATP biosensor, we show that ATP concentrations decrease in the somas of brain neurons during aging due to a reduction in glycolysis or glucose availability. Increased neuronal glucose uptake by expression of a glucose transporter *hGlut3* is sufficient to ameliorate age-dependent declines in ATP via glycolysis. Of particular interest, we demonstrate that increasing glucose uptake into neurons significantly

[1]Department of Biological Sciences, Graduate School of Science, Tokyo Metropolitan University, Tokyo, Japan

[2]Department of Biological Sciences, Faculty of Science, Tokyo Metropolitan University, Tokyo, Japan

[3]Gene Network Laboratory, National Institute of Genetics, Mishima, Shizuoka, Japan

[4]Department of Genetics, SOKENDAI, Mishima, Shizuoka, Japan

[5]Department of Alzheimer's Disease Research, National Center for Geriatrics and Gerontology, Obu, Aichi, Japan

[6]Department of Experimental Gerontology, Graduate School of Pharmaceutical Sciences, Nagoya City University, Nagoya, Aichi, Japan

[7]Lead contact

*Correspondence: k_ando@tmu.ac.jp

https://doi.org/10.1016/j.isci.2020.101979

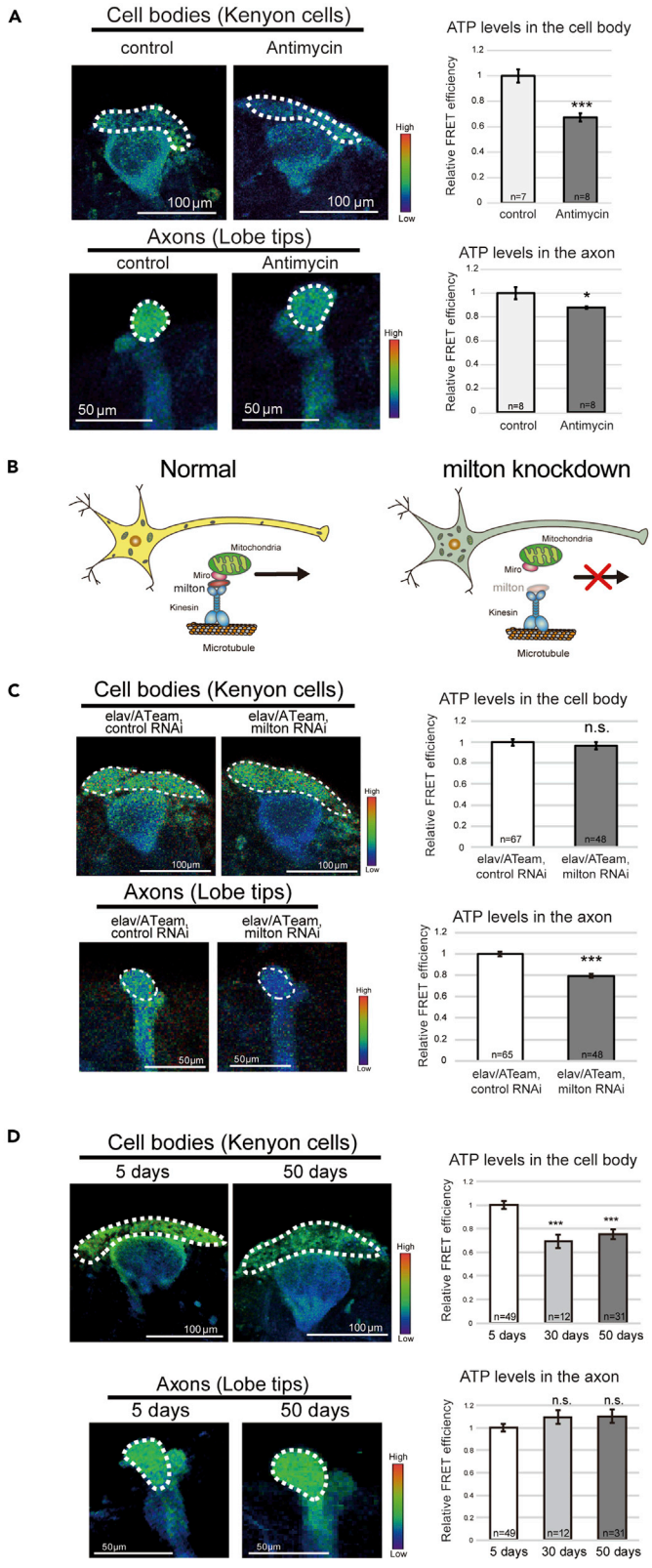
A
Cell bodies (Kenyon cells)
control
Antimycin
100 µm
High
Low
ATP levels in the cell body
Relative FRET efficiency
***
n=7
n=8
control
Antimycin
Axons (Lobe tips)
50 µm
ATP levels in the axon
*
B
Normal
milton knockdown
Mitochondria
Miro
milton
Kinesin
Microtubule
C
Cell bodies (Kenyon cells)
elav/ATeam, control RNAi
elav/ATeam, milton RNAi
n.s.
n=67
n=48
Axons (Lobe tips)
n=65
D
Cell bodies (Kenyon cells)
5 days
50 days
n=49
n=12
n=31
30 days
Axons (Lobe tips)

Figure 1. ATP concentration decreases in the cell body but not in the axon during aging

(A) A reduction in ATP concentration, caused by the inhibition of mitochondrial respiration by antimycin in adult fly brain neurons, was identified using ATeam. ATeam expression was driven by the pan-neuronal driver elav-GAL4. Quantification of the FRET signal (right panels) is shown (mean ± standard error [SE], n = 7–8; *p < 0.05, ***p < 0.001; Student's *t*-test).

(B) Schematic representation of mitochondrial transport. The knockdown of milton, an adapter protein for mitochondrial transport, depleted mitochondria in the axon.

(C) Neuronal knockdown of milton reduced ATP concentration in Kenyon cells and lobe tips. Flies carrying the driver with control RNAi (elav/ATeam, control RNAi) were used as controls. Data are mean ± SE, n = 48–65; not significant (n.s.), p > 0.05, ***p < 0.001; Student's *t*-test).

(D) The FRET efficiency of ATeam in Kenyon cells (A) and lobe tips (B) of the mushroom body of 5-, 30-, and 50-day-old flies (n = 12–49; n.s., p > 0.05, ***p < 0.001; one-way analysis of variance (ANOVA), followed by Tukey's HSD multiple comparisons test). ATeam expression was driven in neurons by the pan-neuronal driver Elav-GAL4.

extends the organismal life span under DR conditions, suggesting that increasing neuronal glucose metabolism optimizes the anti-aging effects of energetic challenges.

RESULTS

An ATP biosensor (ATeam) identifies local changes in ATP levels in *Drosophila* brain neurons

Neurons are highly polarized structurally and functionally and require tight local management of ATP production (Rangaraju et al., 2014). To determine the local ATP concentration in fly brain neurons, we used the fluorescence resonance energy transfer (FRET)-based ATP biosensor, ATeam (Tsuyama et al., 2013). ATeam detects changes in ATP concentrations in the range of 0.5–4 mM at 25°C (Tsuyama et al., 2013, 2017), which is appropriate for the physiological ATP concentrations in neurons (Erecinska and Silver, 1989; Pathak et al., 2015; Rangaraju et al., 2014). The concentrations of intracellular ATP are much higher than the expression levels of ATeam; therefore, the FRET signal derived from ATeam is not likely to be affected by its intracellular distribution (Tsuyama et al., 2013, 2017).

It has been reported that the ATeam signal decreases in response to the inhibition of cellular respiration in the neurons of *Drosophila* larvae (Tsuyama et al., 2013, 2017). To confirm that ATeam is capable of detecting changes in ATP concentration in adult fly brains, we used the Gal4-UAS system to express ATeam in neurons under the control of a pan-neuronal driver elav-GAL4 and inhibited respiratory complex III by treatment with antimycin (AM). We focused on the mushroom body, where axons, dendrites, and cell bodies are easily identifiable as lobes, calyxes, and Kenyon cells, respectively. AM treatment significantly reduced the FRET signal from ATeam in both the cell bodies and axons (Figure 1A), which indicates that ATeam can identify reductions in ATP concentrations in fly brain neurons.

Next, we determined whether ATeam could identify local changes in ATP concentration. To reduce ATP concentration in the axons only, axonal mitochondria were genetically depleted by knocking down milton, an adapter protein for the kinesin motor that is essential for mitochondrial anterograde transport (Figure 1B) (Stowers et al., 2002). Previously, RNAi-mediated neuronal knockdown of milton was reported to effectively deplete mitochondria in axons (Iijima-Ando et al., 2012). Likewise, we found the FRET signal from ATeam decreased in axons but not in the cell bodies of milton-deficient fly brain neurons (Figure 1C). These results indicate that ATeam is capable of identifying local changes in ATP concentration in adult brain neurons.

ATP concentration decreases in the cell body but not in the axon of brain neurons during aging

To determine whether ATP concentration changes in brain neurons in an age-related manner, we compared the ATP concentrations in the mushroom body structure of young (5-day-old), middle-aged (30-day-old), and old (50-day-old) flies. We found that the ATP concentration in the cell bodies in the mushroom body structure of middle-aged (30-day-old) and old (50-day-old) flies was ~70% of that in young flies (5-day-old) (Figure 1D). By contrast, there were no significant changes in axonal ATP concentrations during aging (Figure 1D). ATeam detects ATP levels as cyan fluorescent protein (CFP) and yellow fluorescent protein (YFP) signal ratio, suggesting that the reduction in ATeam signal was not due to the loss of neurons. To confirm this, we carried out immunostaining of the neuronal marker elav and ultrastructural analyses of mushroom body region with electron microscopy. There were no vacuoles or signs of neuronal loss (Figure S1), indicating that the brains of 50-day-old flies were structurally intact, as previously reported (He and Jasper, 2014; Tonoki and Davis, 2015; White et al., 2010). Taken together, these results show that the ATP concentration, specifically in the cell bodies of brain neurons, decreases during aging.

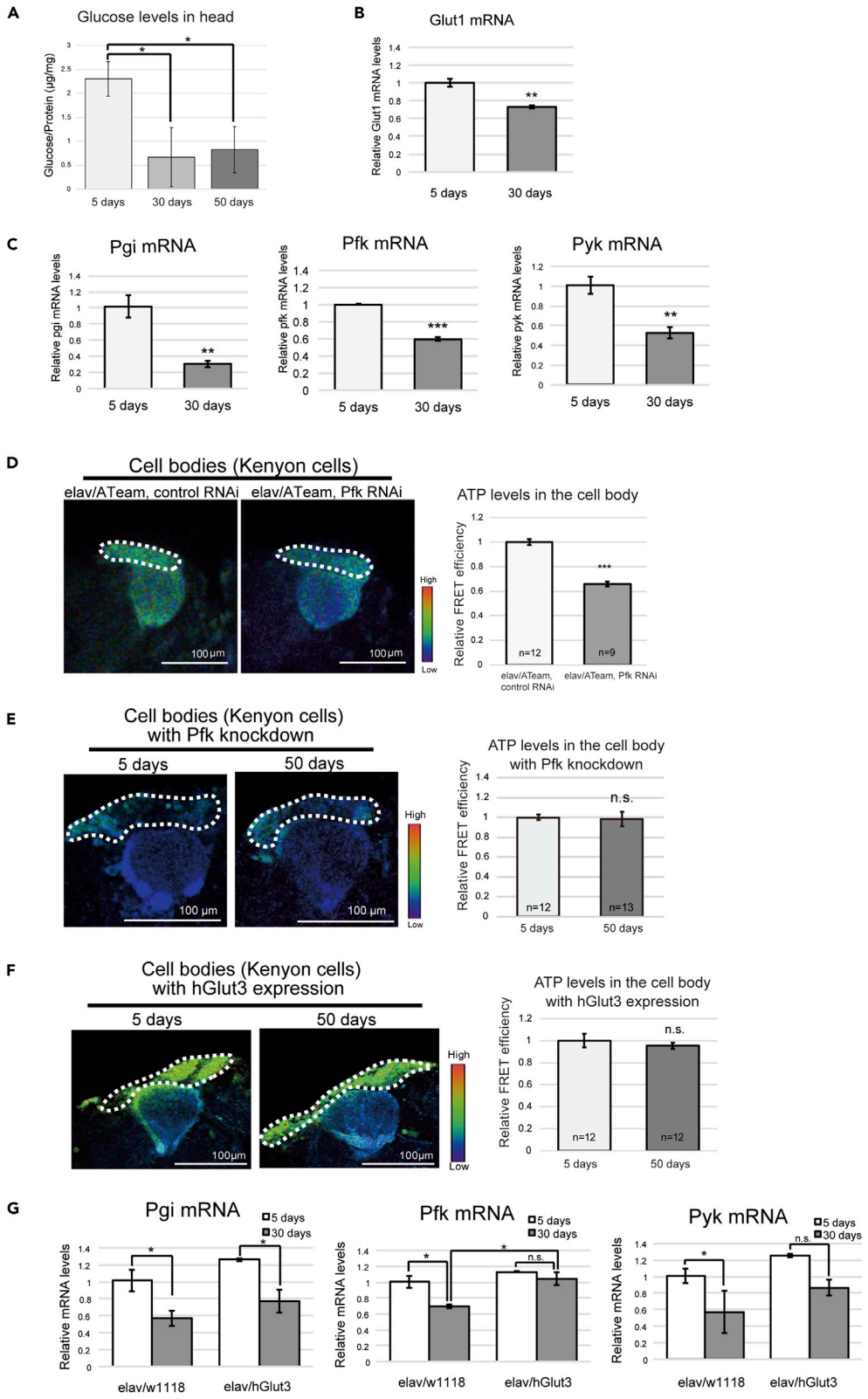
A
Glucose levels in head
Glucose/Protein (μg/mg)
5 days
30 days
50 days
B
Glut1 mRNA
Relative Glut1 mRNA levels
5 days
30 days
C
Pgi mRNA
Relative pgi mRNA levels
Pfk mRNA
Relative pfk mRNA levels
Pyk mRNA
Relative pyk mRNA levels
D
Cell bodies (Kenyon cells)
elav/ATeam, control RNAi
elav/ATeam, Pfk RNAi
ATP levels in the cell body
Relative FRET efficiency
n=12
n=9
E
Cell bodies (Kenyon cells)
with Pfk knockdown
ATP levels in the cell body
with Pfk knockdown
n.s.
n=13
F
Cell bodies (Kenyon cells)
with hGlut3 expression
ATP levels in the cell body
with hGlut3 expression
G
Relative mRNA levels
elav/w1118
elav/hGlut3

Figure 2. Neuronal expression of the glucose transporter *hGlut3* attenuates the age-related reduction in ATP concentration in brain neuron and glycolytic gene expression

(A) Glucose concentration in head lysates decreased during aging. The glucose concentrations in 5-, 30- and 50-day-old fly heads, normalized to protein concentration, are shown (mean ± SE, n = 6; *p < 0.05; one-way ANOVA, followed by Tukey's HSD multiple comparisons test).

(B) *dGlut1* mRNA expression decreased in fly heads during aging. qRT-PCR was performed using RNA extracted from the heads of 5- and 30-day-old flies (mean ± SE, n = 3; **p < 0.01; Student's *t*-test).

(C) The expression of glycolytic genes decreased in the fly brain during aging. The mRNA expression of genes encoding glycolytic enzymes in the heads of 5- and 30-day-old flies was quantified using qRT-PCR (mean ± SE, n = 3; **p < 0.01, ***p < 0.001; Student's *t*-test).

(D) Neuronal knockdown of *Pfk*, which encodes a rate-limiting glycolytic enzyme, reduced ATP concentration in 3-day-old fly neurons (mean ± SE, n = 9–12; ***p < 0.001; Student's *t*-test).

(E) The age-related reduction in ATP concentration in neuronal cell bodies was not identified in *Pfk*-deficient neurons. The expression of ATeam and *Pfk* RNAi was driven by the pan-neuronal driver elav-GAL4. The 5-day-old and 50-day-old flies were subjected to imaging analyzes at the same time. The experiments were repeated with timely independent cohorts of flies obtained from different crosses to analyze more than 12 brains for each age. Data are mean ± SE; n.s., p > 0.05, *p < 0.05; Student's *t*-test.

(F and G) Neuronal expression of *hGlut3* ameliorates the age-related reduction in ATP concentration and glycolytic gene expression and the decline in physical function. (F) ATP concentration did not decrease with aging in neurons overexpressing *hGlut3*. Expression of ATeam and hGlut3 was driven by the pan-neuronal driver elav-GAL4. The 5-day-old and 50-day-old flies were subjected to imaging analyzes at the same time. The experiments were repeated with timely independent cohorts of flies obtained from different crosses to analyze more than 12 brains for each age. (mean ± SE; n.s., p > 0.05; Student's *t*-test). (G) Neuronal expression of *hGlut3* attenuated the age-associated decline in glycolytic gene expression. The mRNA expression of genes encoding key glycolytic enzymes was quantified using qRT-PCR in the heads of 5- and 30-day-old flies. Flies carrying the driver alone were used as controls. Data are mean ± SE, n = 3; n.s., p > 0.05, *p < 0.05, **p < 0.01; one-way ANOVA, followed by Tukey's HSD multiple comparisons test.

Decreases in glycolytic gene expression contribute to the age-related reduction in ATP

Most of the ATP produced in the brain is supplied by the metabolism of glucose (Belanger et al., 2011). To gain insight into the underlying reduced ATP concentrations, we measured glucose availability in the brain decreases during aging in *Drosophila*. We found that the glucose concentration in head extracts was significantly lower in aged flies (30- and 50-day-old) than in young (5-day-old) flies (Figure 2A). Glucose uptake by brain neurons is mostly constitutive because the glucose transporter isoforms expressed in neurons in the central nervous system (CNS), Glut1 and Glut3 in mammals and Glut1 in *Drosophila*, are constitutively localized to the plasma membrane and insensitive to insulin (Chintapalli et al., 2007; Flier et al., 1987). We measured *dGlut1* mRNA expression during aging using real-time quantitative PCR (qRT-PCR), which revealed that its expression was slightly but significantly lower in the heads of aged than in those of young flies (Figure 2B).

In human brains, the rate of glycolysis changes during aging (Goyal et al., 2017). To determine the contribution of changes in glycolytic rate to the age-related reduction in ATP in the cell bodies of *Drosophila* brain neurons, we measured the expression of genes encoding the key glycolytic enzymes in young and aged fly heads including glucose-6-phosphate isomerase (*Pgi*), phosphofructokinase (*Pfk*), and pyruvate kinase (*Pyk*). qRT-PCR analysis revealed that the mRNA expression of *Pgi*, *Pfk*, and *Pyk* was significantly lower in aged flies than in young flies (Figure 2C). To evaluate the contribution of glycolysis to ATP production in brain neurons, we knocked down *Pfk*, which encodes phosphofructokinase, a rate-limiting enzyme in glycolysis. Neuronal knockdown of *Pfk* reduced ATP concentration by up to 65% in 3-day-old flies (Figure 2D), indicating that glycolysis plays a critical role in ATP production in brain neurons. To determine whether the decline in glycolytic activity contributes to the age-related decrease in ATP concentration, we measured the ATeam signal in *Pfk*-deficient young and aged brain neurons. The neurons of 5-day-old flies with *Pfk* knockdown showed a reduced ATP concentration, with no further reduction in 50-day-old flies (Figure 2E). This result suggests that a lower rate of glycolysis and/or events upstream of glycolysis are responsible for the age-related reduction in ATP in cell bodies of brain neurons.

Neuronal expression of the glucose transporter hGlut3 attenuates the age-related reduction in ATP concentration in brain neurons and glycolytic gene expression

We next asked whether increasing glucose uptake could ameliorate the age-related reduction in ATP in the brain neurons. Expression of *hGlut3* in *Drosophila* cells has been reported to increase glucose uptake (Besson et al., 2015). We found that neuronal expression of *hGlut3* ameliorated the age-related reduction in ATP in the neuronal cell bodies (Figure 2F). By contrast, neuronal expression of *hGlut3* did not increase

the ATP concentration in young flies (Figure S2). These results suggest that glucose availability is the rate-limiting factor specifically in the brain neurons of old flies and that overexpression of glucose transporter can increase ATP production in the neurons of aged flies.

We also examined whether glucose transporter overexpression attenuates the age-related changes in glycolytic activity. We found that neuronal expression of *hGlut3* suppressed the age-related decrease in the mRNA expression of the glycolytic gene, *Pfk* (Figure 2G). Taken together, these results suggest that neuronal overexpression of *hGlut3* ameliorates age-related declines in ATP concentration by increasing glucose metabolism in aged fly neurons.

The age-related increase in abnormal mitochondria is not reversed by overexpression of glucose transporter in neurons

Since mitochondrial dysfunction is implicated in aged brains, we examined whether the reduced number and increased damage to mitochondrial was associated with an age-related reduction in ATP levels in brain neurons. We first measured the mitochondrial density in the brain neurons of young and aged flies by transmission electron microscopy. In the cell body, where ATP concentrations decrease (Figure 1D), the number of mitochondria did not change significantly during aging (Figure 3A). Thus, the age-related reduction in ATP in the cell bodies of neurons was not the result of a decrease in the number of mitochondria.

Next, we analyzed the quality of mitochondria in the brain neurons of young and aged flies. Dysfunctional mitochondria are recognized by the abnormal structure of their cristae (Brandt et al., 2017; Daum et al., 2013). Ultrastructural analyses of the mitochondria revealed that the number of abnormal mitochondria in cell bodies slightly but significantly increased during aging (7% in 7-day-old flies and 13% in 35-day-old flies, Figure 3B). By contrast, in the axon, where ATP concentration does not decrease (Figure 1D), the number of mitochondria decreased slightly, but the number of abnormal mitochondria did not significantly change during aging (Figure S3), which might be because of the presence of a robust quality control system in this location (Lin et al., 2017). These results indicate that a slight but significant increase in the number of damaged mitochondria occurs alongside a decrease in ATP concentration in the cell bodies of neurons during aging.

Interestingly, while neuronal overexpression of *hGlut3* ameliorated the age-related reduction in ATP in the neuronal cell bodies (Figure 2F), it neither increased the number of total mitochondria nor reduced the ratio of abnormal mitochondria (Figure 3C). These results suggest that increasing glucose uptake is sufficient to ameliorate energetic deficits in aged brain neurons.

Increasing neuronal glucose uptake ameliorates declines in physical performance in aged flies and has an additive effect with DR in extending life span

Finally, we examined whether the increase in glucose uptake into neurons promoted the health and life span of flies. We first analyzed the effects of neuronal overexpression of *hGlut3* on the age-related decline in physical function using a climbing assay, a robust behavioral assay taking advantage of the innate negative geotaxis behavior. In wild-type flies, climbing ability declined by 45 days of age, whereas flies with neuronal expression of *hGlut3* performed significantly better at this age (Figure 4A), indicating that the increase in glucose uptake into neurons promoted health span in flies. We also found that flies with neuronal expression of *hGlut3* lived slightly but significantly longer than control flies (Figure 4B).

DR has been reported to extend the life span in most species, including *Drosophila* (Bauer et al., 2005). Since DR causes circulating glucose concentrations to fall (Guarente, 2008), the anti-aging effects of DR and increasing in glucose uptake into neurons might be independent and additive. To determine the relationship between neuronal uptake of glucose and DR in aging, we analyzed the effects of neuronal expression of *hGlut3* on life span under various dietary conditions. Flies were raised on regular cornmeal food, and after eclosion, they were fed regular food, DR food (10%) (10% yeast, 10% glucose, no cornmeal), or DR food (1%) (1% yeast, 1% glucose, no cornmeal). Flies on DR food showed reduced levels of glucose in the head and body with greater effects seen with 1% food than 10% food (Figure S4A). The life span was significantly extended on 1% food (Figure S4B), and life span extension by neuronal expression of *hGlut3* was more prominent under DR conditions. While the median life span on regular food was 55 days in control and 59 days in *hGlut3*-expressing flies maintained on regular food (Figure 4B), on 1% food, the median life span was 59 days in control and 73 days in *hGlut3*-expressing flies (Figure 4D). Maintaining flies on 10%

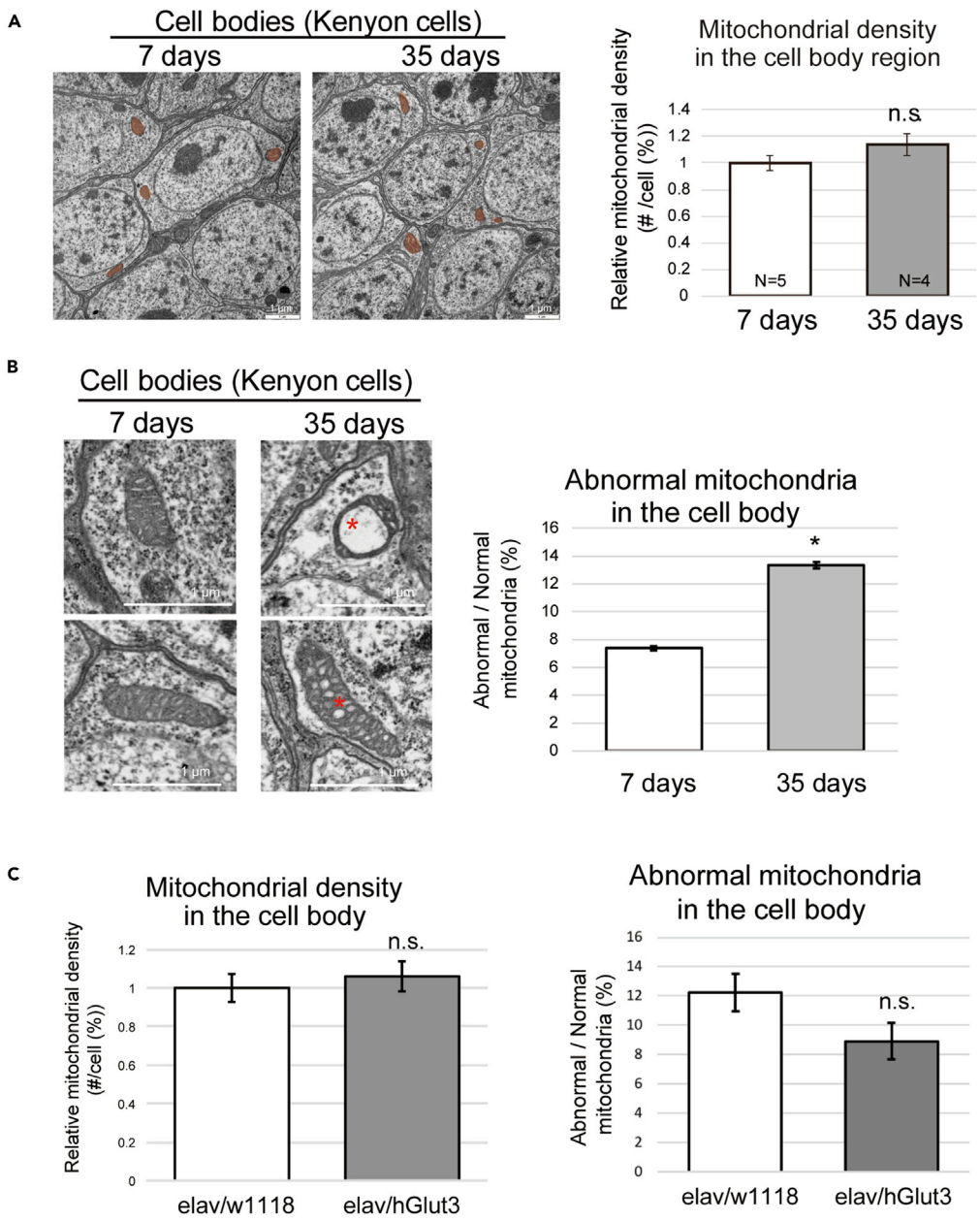

Figure 3. Age-related changes in the number and quality of mitochondria in brain neurons

(A) The number of mitochondria in the neuronal cell body did not significantly change during aging. More than four brain hemispheres from flies of each age were analyzed using transmission electron microscopy (TEM), and the numbers of mitochondria in more than 30 cells in each hemisphere were counted. Representative images are shown, with the mitochondria highlighted in orange.

(B) The ratio of the number of abnormal mitochondria to the total number of mitochondria increased in the cell body during aging. More than four brain hemispheres from flies of each age were examined using TEM, and more than 30 cells were analyzed in each hemisphere. The number of mitochondria containing vacuoles or disorganized cristae (asterisks) was counted. (mean ± SE, n = 4–5; n.s., $p > 0.05$, *$p < 0.05$; Student's t-test).

(C) Neuronal overexpression of *hGlut3* did not affect the age-associated changes in mitochondria in the brain. The mitochondrial density (left) and the ratio of the number of abnormal mitochondria to the total number of mitochondria (right) in neurons expressing *hGlut3* in the Kenyon cell region of the brains were analyzed under TEM 50 days after eclosion (mean ± SE, n = 4–6; n.s., $p > 0.05$; Student's t-test).

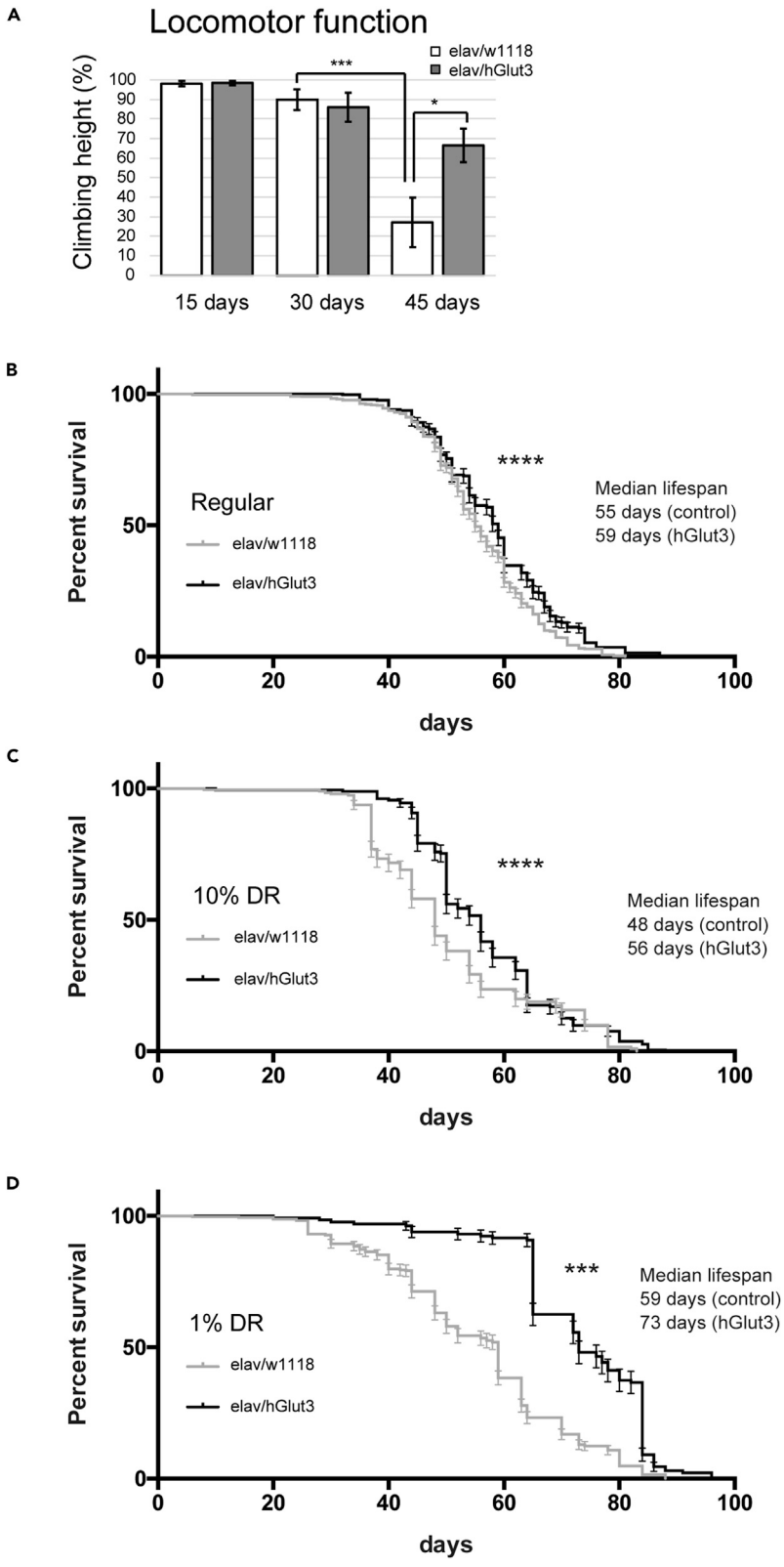
A
Locomotor function
elav/w1118
elav/hGlut3
***
*
Climbing height (%)
100
90
80
70
60
50
40
30
20
10
0
15 days
30 days
45 days
B
Percent survival
Regular
elav/w1118
elav/hGlut3
****
Median lifespan
55 days (control)
59 days (hGlut3)
days
C
Percent survival
10% DR
elav/w1118
elav/hGlut3
****
Median lifespan
48 days (control)
56 days (hGlut3)
days
D
Percent survival
1% DR
elav/w1118
elav/hGlut3
***
Median lifespan
59 days (control)
73 days (hGlut3)
days

Figure 4. Increasing neuronal glucose uptake attenuates declines in physical performance in aged flies and has an additive effect with dietary restriction (DR) in extending life span

(A) Neuronal expression of *hGlut3* ameliorated the age-associated neuronal dysfunction. Flies were tapped to the bottom of the vial, and the distance that they then climbed in 30 s was measured (mean ± SE, n = 12–39; *p < 0.05, ***p < 0.001; Student's *t*-test). Flies carrying the driver alone were used as controls.

(B–D) Neuronal expression of *hGlut3* and DR synergistically extended life span. Flies were raised on regular cornmeal food and maintained on regular cornmeal food (B) or two types of DR diet (C and D) (C: food without cornmeal and containing 10% (w/v) of yeast and glucose (10%), D: food without cornmeal and containing 1% (w/v) of yeast and glucose (1%) after eclosion. Error bars represent 95% confidence intervals. Data are expressed as mean ± SE, n = 131-601, ***; p < 0.001, ****; p < 0.0001, log-rank test.

food did not affect the life span of control flies, but it extended the life span of *hGlut3*-expressing flies (median life span 48 days in control and 56 days in *hGlut3*-expressing flies (Figure 4C)).

We also analyzed glucose levels after *hGlut3* expression in the aged flies under normal and DR conditions. We found that *hGlut3* expression in neurons did not restore glucose levels in aged flies under normal or DR conditions (Figure S5). This result suggests that life span extension caused by neuronal expression of *hGlut3* is not due to gross changes in total levels of glucose in the brain but is associated with efficient uptake of glucose and its utilization in neurons. When glucose availability is limited under DR conditions, efficiency of glucose utilization would have more impact than under normal conditions. Enhancement of glucose uptake by overexpression of *hGlut3* may, therefore, be prominent under DR conditions. Taken together, these results suggest that increased glucose uptake by neurons enhances the anti-aging effects of DR at the organismal level.

DISCUSSION

In the present study, we showed that aged brain neurons suffer from energy deficits, along with decreases in glucose concentration, the expression levels of glucose transporter and glycolytic enzymes (Figures 1 and 2), and mitochondrial quality (Figure 3). Increasing glucose uptake by neurons was sufficient to attenuate energetic deficits (Figure 2) despite persistent mitochondrial damage (Figure 3) and suppressed age-dependent locomotor decline (Figure 4). Interestingly, the effects of increasing glucose uptake on life span extension were more prominent under DR (Figures 4B–4D), suggesting that increasing neuronal uptake of glucose in concert with bioenergetic challenges could benefit health and life span in flies.

During aging, the ATP supply to brain neurons decreases because of global reductions in glucose metabolism, including in oxygen consumption, glycolysis, and mitochondrial respiratory capacity (Conley et al., 2000; Goyal et al., 2017; Jang et al., 2018; Kety, 1956; Martin et al., 1991). Our results suggest that glucose uptake was a limiting factor for ATP supply in aged brain neurons. An increase in glucose uptake attenuated not only the reduction in neuronal ATP concentration during aging but also the age-related reduction in the expression of glycolytic enzymes (Figure 2). In mammalian cells, it has been reported that an elevated concentration of intracellular glucose activates hypoxia-inducible factor-1α (Guo et al., 2008), which promotes the expression of glycolytic enzymes (Lum et al., 2007). An increase in glucose uptake did not suppress the age-related reduction in mitochondrial quality (Figure 3), suggesting that enhanced glucose supply can produce sufficient ATP despite mitochondrial damage to produce sufficient ATP *in vivo*.

DR is known to extend life span in many species, but it may reduce glucose supply to the brain and worsen energy deficits in neurons. We used DR conditions that are similar to Bauer et al. (Bauer et al., 2005), under which both the levels of sugar and yeast are reduced. Unlike Bauer et al., we saw an initial increase in mortality followed by a prolongation of life span (Figure S4), although the extension of life span was less than that observed in previous works (Bauer et al., 2005; Bross et al., 2005). This difference may be due to different laboratory media used to maintain stocks. The food used in our facility is relatively rich in yeast and cornmeal (4% yeast, 10% glucose, 9% cornmeal) compared with that used by Bauer et al. (2% yeast, 10% sucrose, 5% cornmeal); this difference may have affected the response to DR in the studied offspring.

Our results suggest that increased glucose uptake by neurons further improves the anti-aging effects of DR, presumably by counteracting neuronal energy deficits under DR conditions (Figure 4). Lower extracellular glucose caused by DR may recapitulate some of the conditions observed in the aged brain, in which lower cerebral blood flow limits glucose supply (Goyal et al., 2017; Hoyer, 2000; Noda et al., 2002). In

Drosophila, life span extension by DR is mostly modulated by dietary yeast (Grandison et al., 2009; Lee et al., 2008; Mair et al., 2005): DR in *Drosophila* research is often performed simply by reducing the amount of yeast. In this study, both sugar and yeast were reduced in the DR condition, which caused a reduction in overall glucose availability (Figure S4). One might suspect that a reduction in sugar would have a negative effect on survival and *hGlut3* overexpression simply restored glucose availability. However, the glucose content in the head was not restored by neuronal expression of *hGlut3* (Figure S5), suggesting this was not the case. Instead, our results suggest that enhancing neuronal glucose uptake had more impact under conditions in which glucose availability is limited. In support of this, a previous study that did not use DR showed no effect of neuronal expression of *dGlut1* or *hGlut3* on life span (Besson et al., 2015; Niccoli et al., 2016).

The anti-aging effects of DR are reported to be mediated by a reduction in the intake of protein or amino acids (Mirzaei et al., 2014). Amino acid restriction affects life span through effects on amino acid sensing pathways, such as mechanistic target of rapamycin complex 1 and the integrated stress response (Mirzaei et al., 2014). The additive effects of DR and neuronal expression of *hGlut3* on life span may be explained by the respective peripheral activation of anti-aging pathways by DR and increased neuronal glucose uptake and metabolism. Thus, a strategy aimed at both increasing glucose uptake by neurons and restricting amino acid intake may be effective at reducing the effects of aging.

In summary, we have shown that glucose uptake by brain neurons is a critical regulator of organismal and brain aging. Further elucidation of the cross-talk among nutrient signaling pathways in the central nervous system and peripheral tissues during aging will lead to the identification of novel strategies for the extension of the healthy life span of an organism.

Limitations of the study

We demonstrated that increased glucose uptake in neurons further extends life span under a DR condition. We used a DR protocol with a reduction in total calories. Since it has been reported that specific nutrients and their relative ratios play roles in their effects on life span extension (Mirzaei et al., 2014), it would be interesting to test the effects of neuronal expression of hGlut3 under other dietary conditions, such as limiting specific nutrients. In this study, we expressed hGlut3 in all neurons using a pan-neuronal elav-Gal4 driver and did not analyze the effect of increasing glucose uptake in specific types of neurons, glial cells, or in the other non-neuronal tissues on life span. Such experiments will elucidate cell type- and tissue-specific roles of glucose metabolism in aging and life span. We showed that increasing neuronal glucose uptake counteracts their age-dependent reduction in *pfk* expression, while the mechanism by which increasing intracellular glucose affects glycolytic gene expression remains unknown. Our analysis on the age-dependent change in mitochondrial quality was limited to the ultrastructural analysis, and mitochondrial functions were not analyzed. We hope to address these issues in the future for better understanding of the multifactorial processes of aging.

Resource availability

Lead contact

Further information and requests for resources and reagents should be directed to and will be fulfilled by the Lead Contact, Kanae Ando (k_ando@tmu.ac.jp).

Material availability

This study did not generate new materials.

Data and code availability

This study did not generate data sets or analyze codes.

METHODS

All methods can be found in the accompanying Transparent methods supplemental file.

SUPPLEMENTAL INFORMATION

Supplemental information can be found online at https://doi.org/10.1016/j.isci.2020.101979.

ACKNOWLEDGMENT

The authors thank Dr. Hiromi Imamura from the Graduate School of Biostudies, Kyoto University, for the ATP biosensor transgenic fly line and discussions. The authors thank Dr. Marie Thérèse Besson, Aix-Marseille Université, for UAS-hGlut3 fly line. The authors are grateful to Dr. Shin-ichi Hisanaga from the Department of Biological Sciences, Tokyo Metropolitan University, for critical comments. The authors thank Tetsuya Miyashita for technical support. This work was supported by a research award from the Japan Foundation for Aging and Health (to K.A) and a Grant-in-Aid for Scientific Research on Challenging Research (Exploratory) [JSPS KAKENHI Grant number 19K21593] (to K.A.), NIG-JOINT (71A2018, 25A2019) (to K.A.), and [JSPS Grant-in-Aid for JSPS Research Fellow 18J21936] (to M.O.), and the Research Funding for Longevity Science 19-7 from the National Center for Geriatrics and Gerontology, Japan (to K.M.I.).

AUTHOR CONTRIBUTION

M.O., K.M.I., and K.A. designed the experiments, interpreted the data, and wrote the manuscript; M.O., A.A., T.S., and E.S. conducted the experiments; and M.O., E.S., and K.A. analyzed the data. All authors read and approved the manuscript.

DECLARATION OF INTERESTS

The authors declare no competing interests.

Received: May 20, 2020
Revised: October 29, 2020
Accepted: December 17, 2020
Published: January 22, 2021

REFERENCES

Alcedo, J., and Kenyon, C. (2004). Regulation of C. elegans longevity by specific gustatory and olfactory neurons. Neuron *41*, 45–55.

Bauer, J.H., Poon, P.C., Glatt-Deeley, H., Abrams, J.M., and Helfand, S.L. (2005). Neuronal expression of p53 dominant-negative proteins in adult Drosophila melanogaster extends life span. Curr. Biol. *15*, 2063–2068.

Belanger, M., Allaman, I., and Magistretti, P.J. (2011). Brain energy metabolism: focus on astrocyte-neuron metabolic cooperation. Cell Metab. *14*, 724–738.

Besson, M.T., Alegria, K., Garrido-Gerter, P., Barros, L.F., and Lievens, J.C. (2015). Enhanced neuronal glucose transporter expression reveals metabolic choice in a HD Drosophila model. PLoS One *10*, e0118765.

Brandt, T., Mourier, A., Tain, L.S., Partridge, L., Larsson, N.G., and Kuhlbrandt, W. (2017). Changes of mitochondrial ultrastructure and function during ageing in mice and Drosophila. Elife *6*, e24662.

Bross, T.G., Rogina, B., and Helfand, S.L. (2005). Behavioral, physical, and demographic changes in Drosophila populations through dietary restriction. Aging Cell *4*, 309–317.

Burkewitz, K., Morantte, I., Weir, H.J.M., Yeo, R., Zhang, Y., Huynh, F.K., Ilkayeva, O.R., Hirschey, M.D., Grant, A.R., and Mair, W.B. (2015). Neuronal CRTC-1 governs systemic mitochondrial metabolism and lifespan via a catecholamine signal. Cell *160*, 842–855.

Chintapalli, V.R., Wang, J., and Dow, J.A. (2007). Using FlyAtlas to identify better Drosophila melanogaster models of human disease. Nat. Genet. *39*, 715–720.

Cohen, D.E., Supinski, A.M., Bonkowski, M.S., Donmez, G., and Guarente, L.P. (2009). Neuronal SIRT1 regulates endocrine and behavioral responses to calorie restriction. Genes Dev. *23*, 2812–2817.

Conley, K.E., Jubrias, S.A., and Esselman, P.C. (2000). Oxidative capacity and ageing in human muscle. J. Physiol. *526* (Pt 1), 203–210.

Daum, B., Walter, A., Horst, A., Osiewacz, H.D., and Kuhlbrandt, W. (2013). Age-dependent dissociation of ATP synthase dimers and loss of inner-membrane cristae in mitochondria. Proc. Natl. Acad. Sci. U S A *110*, 15301–15306.

Erecinska, M., and Silver, I.A. (1989). ATP and brain function. J. Cereb. Blood Flow Metab. *9*, 2–19.

Flier, J.S., Mueckler, M.M., Usher, P., and Lodish, H.F. (1987). Elevated levels of glucose transport and transporter messenger RNA are induced by ras or src oncogenes. Science *235*, 1492–1495.

Goyal, M.S., Vlassenko, A.G., Blazey, T.M., Su, Y., Couture, L.E., Durbin, T.J., Bateman, R.J., Benzinger, T.L., Morris, J.C., and Raichle, M.E. (2017). Loss of brain aerobic glycolysis in normal human aging. Cell Metab. *26*, 353–360.e3.

Grandison, R.C., Piper, M.D., and Partridge, L. (2009). Amino-acid imbalance explains extension of lifespan by dietary restriction in Drosophila. Nature *462*, 1061–1064.

Guarente, L. (2008). Mitochondria–a nexus for aging, calorie restriction, and sirtuins? Cell *132*, 171–176.

Guo, S., Bragina, O., Xu, Y., Cao, Z., Chen, H., Zhou, B., Morgan, M., Lin, Y., Jiang, B.H., Liu, K.J., et al. (2008). Glucose up-regulates HIF-1 alpha expression in primary cortical neurons in response to hypoxia through maintaining cellular redox status. J. Neurochem. *105*, 1849–1860.

He, Y., and Jasper, H. (2014). Studying aging in Drosophila. Methods *68*, 129–133.

Hoyer, S. (2000). Brain glucose and energy metabolism abnormalities in sporadic Alzheimer disease. Causes and consequences: an update. Exp. Gerontol. *35*, 1363–1372.

Iijima-Ando, K., Sekiya, M., Maruko-Otake, A., Ohtake, Y., Suzuki, E., Lu, B., and Iijima, K.M. (2012). Loss of axonal mitochondria promotes tau-mediated neurodegeneration and Alzheimer's disease-related tau phosphorylation via PAR-1. PLoS Genet. *8*, e1002918.

Jang, J.Y., Blum, A., Liu, J., and Finkel, T. (2018). The role of mitochondria in aging. J. Clin. Invest. *128*, 3662–3670.

Kety, S.S. (1956). Human cerebral blood flow and oxygen consumption as related to aging. J. Chronic Dis. *3*, 478–486.

Kirkwood, T.B., and Austad, S.N. (2000). Why do we age? Nature *408*, 233–238.

Lee, K.P., Simpson, S.J., Clissold, F.J., Brooks, R., Ballard, J.W., Taylor, P.W., Soran, N., and Raubenheimer, D. (2008). Lifespan and

reproduction in Drosophila: new insights from nutritional geometry. Proc. Natl. Acad. Sci. U S A *105*, 2498–2503.

Libert, S., Zwiener, J., Chu, X., Vanvoorhies, W., Roman, G., and Pletcher, S.D. (2007). Regulation of Drosophila life span by olfaction and food-derived odors. Science *315*, 1133–1137.

Lin, M.Y., Cheng, X.T., Tammineni, P., Xie, Y., Zhou, B., Cai, Q., and Sheng, Z.H. (2017). Releasing syntaphilin removes stressed mitochondria from axons independent of mitophagy under pathophysiological conditions. Neuron *94*, 595–610 e596.

Lum, J.J., Bui, T., Gruber, M., Gordan, J.D., DeBerardinis, R.J., Covello, K.L., Simon, M.C., and Thompson, C.B. (2007). The transcription factor HIF-1alpha plays a critical role in the growth factor-dependent regulation of both aerobic and anaerobic glycolysis. Genes Dev. *21*, 1037–1049.

Mair, W., Piper, M.D., and Partridge, L. (2005). Calories do not explain extension of life span by dietary restriction in Drosophila. PLoS Biol. *3*, e223.

Martin, A.J., Friston, K.J., Colebatch, J.G., and Frackowiak, R.S. (1991). Decreases in regional cerebral blood flow with normal aging. J. Cereb. Blood Flow Metab. *11*, 684–689.

Mink, J.W., Blumenschine, R.J., and Adams, D.B. (1981). Ratio of central nervous system to body metabolism in vertebrates: its constancy and functional basis. Am. J. Physiol. *241*, R203–R212.

Mirzaei, H., Suarez, J.A., and Longo, V.D. (2014). Protein and amino acid restriction, aging and disease: from yeast to humans. Trends Endocrinol. Metab. *25*, 558–566.

Niccoli, T., Cabecinha, M., Tillmann, A., Kerr, F., Wong, C.T., Cardenes, D., Vincent, A.J., Bettedi, L., Li, L., Gronke, S., et al. (2016). Increased glucose transport into neurons rescues abeta toxicity in Drosophila. Curr. Biol. *26*, 2291–2300.

Noda, A., Ohba, H., Kakiuchi, T., Futatsubashi, M., Tsukada, H., and Nishimura, S. (2002). Age-related changes in cerebral blood flow and glucose metabolism in conscious rhesus monkeys. Brain Res. *936*, 76–81.

Pathak, D., Shields, L.Y., Mendelsohn, B.A., Haddad, D., Lin, W., Gerencser, A.A., Kim, H., Brand, M.D., Edwards, R.H., and Nakamura, K. (2015). The role of mitochondrially derived ATP in synaptic vesicle recycling. J. Biol. Chem. *290*, 22325–22336.

Raichle, M.E., Posner, J.B., and Plum, F. (1970). Cerebral blood flow during and after hyperventilation. Arch. Neurol. *23*, 394–403.

Rangaraju, V., Calloway, N., and Ryan, T.A. (2014). Activity-driven local ATP synthesis is required for synaptic function. Cell *156*, 825–835.

Satoh, A., and Imai, S. (2014). Systemic regulation of mammalian ageing and longevity by brain sirtuins. Nat. Commun. *5*, 4211.

Stowers, R.S., Megeath, L.J., Gorska-Andrzejak, J., Meinertzhagen, I.A., and Schwarz, T.L. (2002). Axonal transport of mitochondria to synapses depends on milton, a novel Drosophila protein. Neuron *36*, 1063–1077.

Tonoki, A., and Davis, R.L. (2015). Aging impairs protein-synthesis-dependent long-term memory in Drosophila. J. Neurosci. *35*, 1173–1180.

Tsuyama, T., Kishikawa, J., Han, Y.W., Harada, Y., Tsubouchi, A., Noji, H., Kakizuka, A., Yokoyama, K., Uemura, T., and Imamura, H. (2013). In vivo fluorescent adenosine 5'-triphosphate (ATP) imaging of Drosophila melanogaster and Caenorhabditis elegans by using a genetically encoded fluorescent ATP biosensor optimized for low temperatures. Anal. Chem. *85*, 7889–7896.

Tsuyama, T., Tsubouchi, A., Usui, T., Imamura, H., and Uemura, T. (2017). Mitochondrial dysfunction induces dendritic loss via eIF2alpha phosphorylation. J. Cell Biol. *216*, 815–834.

Ulgherait, M., Rana, A., Rera, M., Graniel, J., and Walker, D.W. (2014). AMPK modulates tissue and organismal aging in a non-cell-autonomous manner. Cell Rep. *8*, 1767–1780.

White, K.E., Humphrey, D.M., and Hirth, F. (2010). The dopaminergic system in the aging brain of Drosophila. Front. Neurosci. *4*, 205.

Zhang, B., Gong, J., Zhang, W., Xiao, R., Liu, J., and Xu, X.Z.S. (2018). Brain-gut communications via distinct neuroendocrine signals bidirectionally regulate longevity in C. elegans. Genes Dev. *32*, 258–270.

iScience, Volume *24*

Supplemental Information

Increasing neuronal glucose uptake attenuates brain aging and promotes life span under dietary restriction in *Drosophila*

Mikiko Oka, Emiko Suzuki, Akiko Asada, Taro Saito, Koichi M. Iijima, and Kanae Ando

Supplemental figure 1

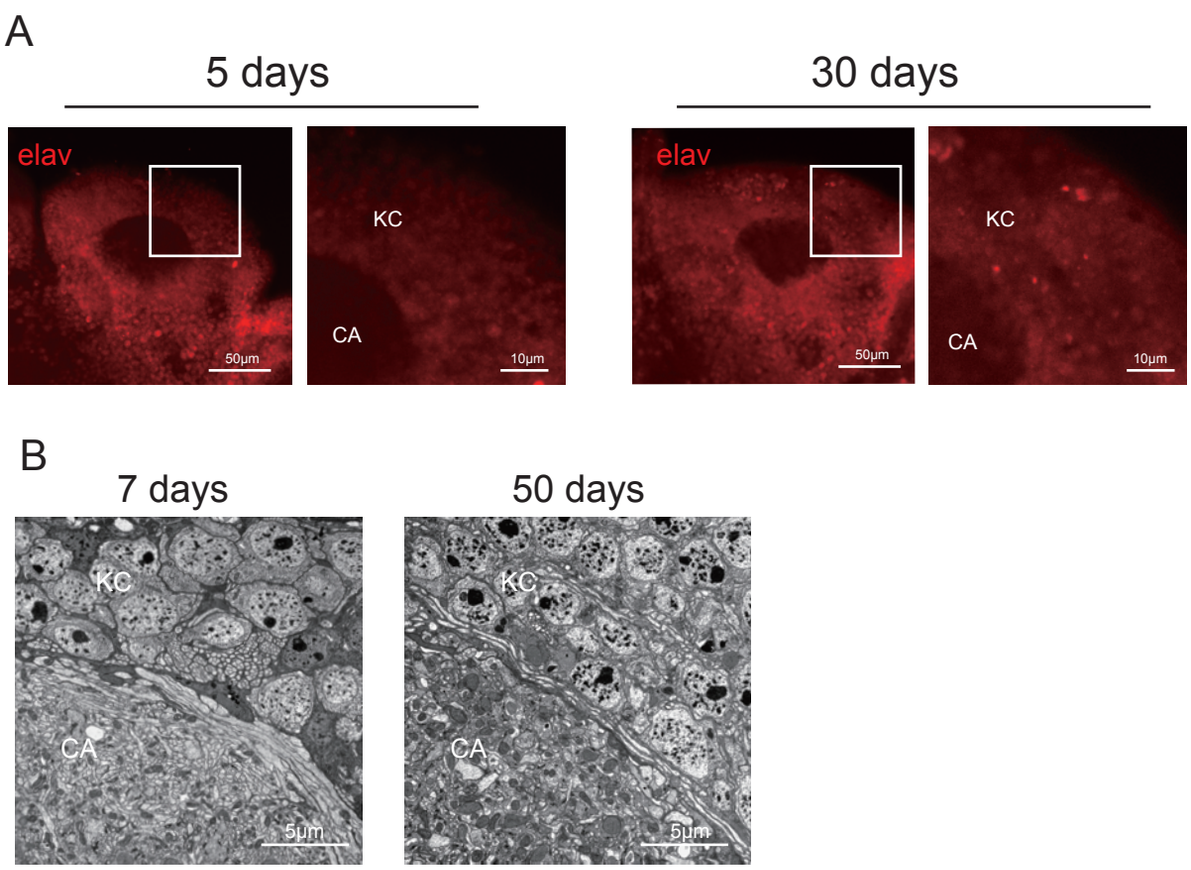

Figure S1. Kenyon cells in aged fly brains are structurally intact, Related to Figure 1

(A) Fly brains expressing an ATP biosensor in neurons were immunostained with an antibody for the neuronal marker elav. Low and high magnification of the maximum intensity projection of Calyx (CA) and Kenyon Cells (KC) are shown. More than six brains were analyzed, and no degeneration was observed. (B) Ultrastructural analyzes of Kenyon cells show no sign of cell death in the aged brains. More than four brain hemispheres from young (7-day-old) and aged (50-day-old) flies were analyzed using transmission electron microscopy (TEM).

Supplemental figure 2

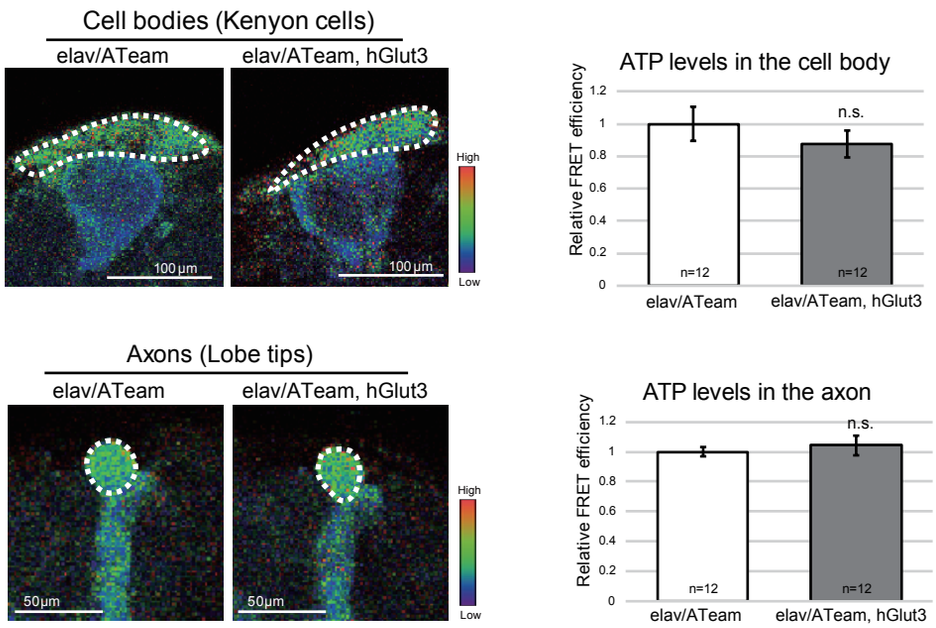

Figure S2. The overexpression of hGlut3 does not increase ATP concentration in the mushroom body neurons of young flies, Related to Figure 2

The FRET signals from ATeam were quantified and are shown as mean ± SE (n=12, n.s.; p>0.05, Student's t-test). The flies were 5 days old.

Supplemental figure 3

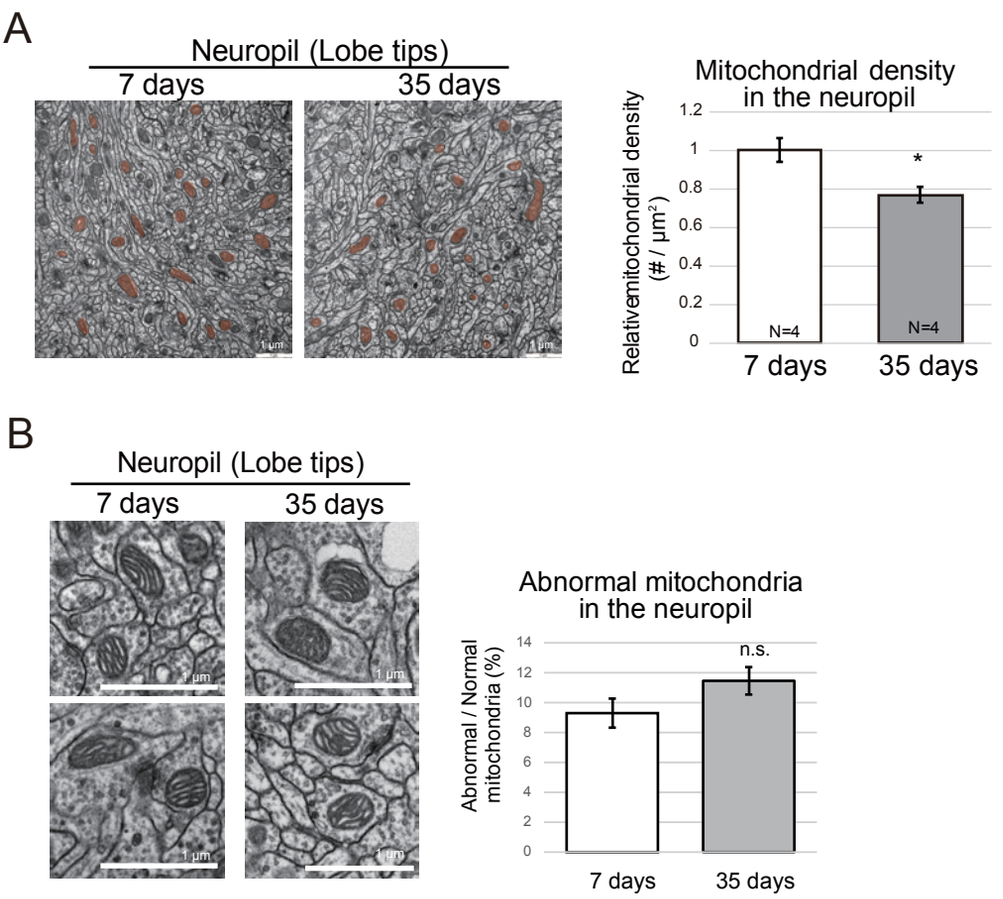

Figure S3. Age-related changes in the number and quality of mitochondria in the axon, Related to Figure 3

(A) The number of mitochondria in the axon significantly decreased during aging. More than four brain hemispheres from flies of each age were analyzed using transmission electron microscopy (TEM), and the numbers of mitochondria in the lobe tip in at least in each hemisphere were counted. Representative images are shown, with the mitochondria highlighted in orange. (B) The ratio of the number of abnormal mitochondria to the total number of mitochondria did not significantly change in the axon during aging. The number of mitochondria containing vacuoles or disorganized cristae was counted. Scale bar: 1 μm. Mean ± SE, n=4–5; n.s., $p>0.05$, *$p<0.05$; Student's t-test.

Supplemental figure 4

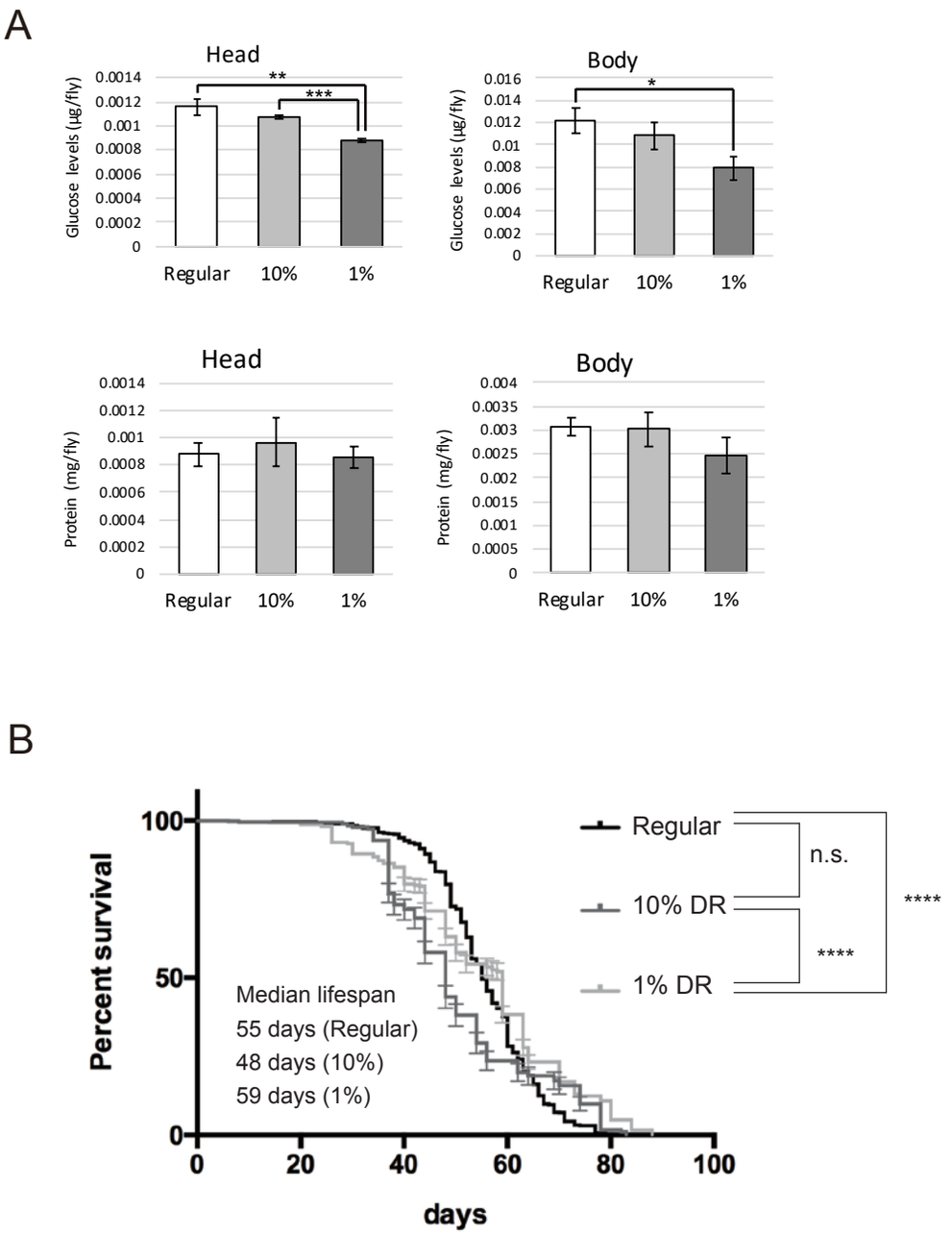

Figure S4. The effects of dietary restriction (DR) on glucose levels and life span, Related to Figure 4

(A) Flies undergoing DR have lower levels of glucose in their heads. The glucose and protein concentrations in the heads of flies subjected to DR. Flies were raised on regular cornmeal food and after eclosion, were maintained on regular corn meal food (Regular) or two types of DR diet (10% and 1%)(10%: food without cornmeal and containing 10% (w/v) of yeast and glucose, 1%: food without cornmeal and containing 1% (w/v) of yeast and glucose). Flies were 30-day-old. Data are mean ± SE, n=3, **; p<0.01, ***; p<0.001, Student's t-test. (B) Flies maintained on 1% food showed longer lifespan. Error bars represent 95% confidence intervals. Data are mean ± SE, n=131-601, n.s.; p>0.05, ****; p

Supplemental figure 5

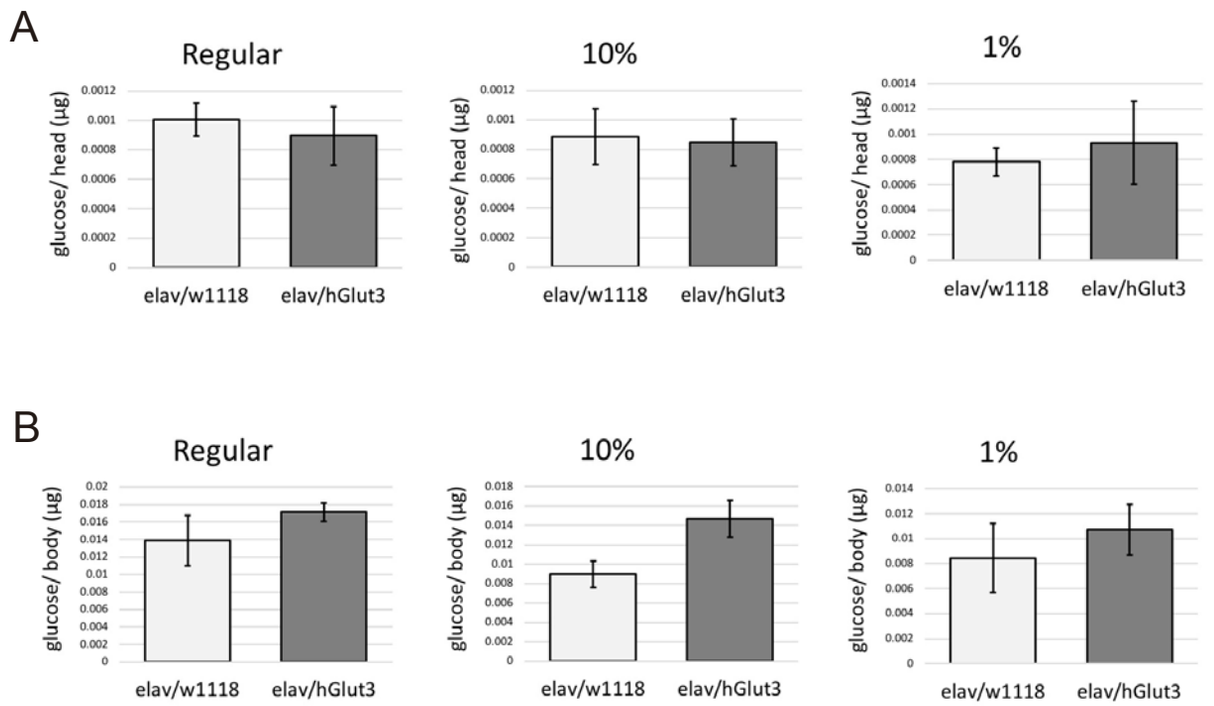

Figure S5. Glucose levels in the head or body were not increased by neuronal expression of hGlut3 under regular or dietary restriction (DR) conditions, Related to Figure 4

Flies were raised on regular cornmeal food and maintained on regular cornmeal food or two types of DR diet (10% and 1%) (10%: food without cornmeal and containing 10% (w/v) of yeast and glucose, 1%: food without cornmeal and containing 1% (w/v) of yeast and glucose) after eclosion. The glucose concentrations in 30-day-old fly heads (A) and bodies (B) are shown (mean ± SE, n=3, Student's t-test, $p>0.05$).

Table S1. The genotypes of flies used in each experiment, Related to Figure 1-4 and Transparent Methods

Figure 1A	control	elav-Gal4/+;;UAS-ATeam/+
Figure 1C	control RNAi	elav-Gal4/+;;UAS-luciferase/UAS-ATeam
	milton RNAi	elav-Gal4/UAS-milton RNAi^{v42508};;UAS-ATeam
Figure 1D	control	elav-Gal4/+;;UAS-ATeam
Figure 2A	control	elav-Gal4/+
Figure 2B	control	elav-Gal4/+
Figure 2C	control	elav-Gal4/+
Figure 2D	control RNAi	elav-Gal4/+;;UAS-luciferase^{B31603}/UAS-ATeam
	pfk RNAi	elav-Gal4/+; UAS-pfk RNAi^{B36782}/+; UAS-ATeam/+
Figure 2E	pfk RNAi	elav-Gal4/+; UAS-pfk RNAi^{v101887}/+; UAS-ATeam/+
Figure 2F	hGlut3	elav-Gal4/+; UAS-hGlut3/+; UAS-ATeam/+
Figure 2G	control	elav-Gal4/+
	hGlut3	elav-Gal4/+; UAS-hGlut3/+
Figure 3A	control	elav-Gal4/+
Figure 3B	control	elav-Gal4/+
Figure 3C	control	elav-Gal4/+
	hGlut3	elav-Gal4/+; hGlut3/+
Figure4A	control	elav-Gal4/+
	hGlut3	elav-Gal4/+; hGlut3/+
Figure4B	control	elav-Gal4/+
	hGlut3	elav-Gal4/+; hGlut3/+
Figure 4C	control	elav-Gal4/+
	hGlut3	elav-Gal4/+; hGlut3/+
Figure 4D	control	elav-Gal4/+
	hGlut3	elav-Gal4/+; hGlut3/+
S1A	control	elav-Gal4/+;;UAS-ATeam/+
S1B	control	elav-Gal4/+
S2	control	elav-Gal4/+;;UAS-ATeam
	hGlut3	elav-Gal4/+; UAS-hGlut3/+; UAS-ATeam/+
S3A	control	elav-Gal4/+
S3B	control	elav-Gal4/+
S4A	control	elav-Gal4/+
S4B	control	elav-Gal4/+
S5	control	elav-Gal4/+
	hGlut3	elav-Gal4/+; hGlut3/+

Transparent Methods

Fly strains

The transgenic fly line carrying UAS-ATeam was a kind gift from Dr. Hiromi Imamura (Kyoto University) (Tsuyama et al., 2013). The transgenic fly line carrying the human Glut3 was reported previously and a kind gift from Dr. Marie Thérèse Besson (Besson et al., 2015). UAS-Pfk RNAi (B36782) and UAS-luciferase RNAi (B31603) were obtained from the Bloomington stock center. UAS-Pfk RNAi (v101887) and RNAi-TK (v60100) as KK RNAi control were obtained from Vienna Drosophila Resource Center (VDRC). UAS-milton RNAi was obtained from VDRC (v41508) and outcrossed to [*w1118*] for five generations in our laboratory. Control flies for Pfk RNAi (Figure 2D) were obtained by crossing elav-GAL4 with UAS-luciferase RNAi (Perkins et al., 2015). Control flies for hGlut3 expression were obtained by crossing elav-GAL4 flies or elav-GAL4;UAS-ATeam flies with the parental strain obtained from the laboratory that generated the UAS-hGlut3 fly line (Besson et al., 2015). Genotypes of the flies used in the experiments are described in Table S1. Flies were reared in a standard medium containing 10% glucose, 0.7% agar, 9% cornmeal, 4% Brewer's yeast, 0.3% propionic acid and 0.1% n-butyl p-hydroxybenzoate [w/v]. Flies were maintained at 25°C under light-dark cycles of 12:12 hours, and food vials were changed every 2-3 days.

FRET imaging and analysis

FRET-based ATP biosensors, ATeams, consist of mseCFP as a FRET donor, cp173-mVenus as a FRET acceptor, and the epsilon subunit of Bacillus subtilis FoF1 ATP-synthase, which links the donor with the acceptor (Imamura et al., 2009). Binding of ATP to the epsilon subunit induces its large conformational change into a folded form, increasing FRET (Imamura et al., 2009). For FRET imaging, flies were kept at 25°C, where the probe is optimized to detect changes in physiologically relevant ATP levels (Tsuyama et al., 2013). Flies expressing ATeam were imaged using C2 confocal microscope (Nikon) with a 440-nm solid-state laser for excitation two emission filters (482±17.5 for CFP and 537±13 for YFP-FRET). A series of z-sections was projected, if necessary. To subtract background signals, a region adjacent to regions of interest (ROIs) was set as background regions. The mean fluorescent intensity of the background regions was subtracted from that of the ROI. FRET signals (FRET/CFP emission ratio) within ROIs were calculated by dividing the mean intensity of FRET emission by that of the CFP emission using Microsoft Excel (Microsoft). Ratio images were generated using NIS-Elements imaging software (Nikon). For imaging of adult brain preparations, brains were dissected in HL3.1 buffer containing 70mM NaCl, 5mM KCl, 0.2mM $CaCl_2$, 20mM $MgCl_2$, 10mM $NaHCO_3$, 5mM Trehalose, 5mM HEPES. To inhibit mitochondrial respiration, dissected brains were treated with 100 μM of Antimycin A (Santa Cruz Biotechnology) for 15 min. The flies were handled in the same incubator and analyzed under the same experimental conditions. The experiments were repeated with timely independent cohorts of flies obtained from different crosses.

Electron microscopy

Proboscis was removed from decapitated heads, which were then incubated in primary fixative solution (2.5% glutaraldehyde and 2% paraformaldehyde in 0.1 M sodium cacodylate buffer) at R.T. for 2 hours. After washing heads with 3% sucrose in 0.1 M sodium cacodylate buffer, fly heads were post-fixed for 1 hour in secondary fixation (1% osmium tetroxide in 0.1 M sodium cacodylate buffer) on ice. After washing with H_2O, heads were dehydrated with ethanol and infiltrated with propylene oxide and Epon mixture (TAAB and Nissin EM) for 3 hours. After infiltration, specimens were embedded with Epon mixture at 70°C for 2~3 days. Thin-sections (70 nm) of mushroom body were collected on copper grids. The sections were stained with 2% uranyl acetate in 70% ethanol and Reynolds' lead citrate solution.

Electron micrographs were obtained with a VELETA CCD Camera (Olympus Soft Imaging Solutions GMBH) mounted on a JEM-1010 electron microscope (Jeol Ltd.).

RNA extraction and quantitative real-time PCR analysis

Heads from more than 25 flies were mechanically isolated, and total RNA was extracted using ISOGEN (NipponGene) followed by reverse-transcription using PrimeScript RT reagent kit (Takara). The resulting cDNA was used as a template for PCR with THUNDERBIRD SYBR qPCR mix (TOYOBO) on a Thermal Cycler Dice real-time system TP800 (Takara). Expression of genes of interest was standardized relative to *rp49*. Relative expression values were determined by the ΔΔCT method (Livak and Schmittgen, 2001). Experiments were repeated three times, and a representative result was shown. Primers were designed using DRSC FlyPrimerBank (Harvard Medical School). Primer sequences are shown below;
Glut1 for 5'-TTACCGCGGAGCTCTTCTCC-3'
Glut1 rev 5'-GCCATCCAGTTGACCAGCAC-3'
Pgi for 5'-AGATACTGCTGGACTACTCGAAG-3'
Pgi rev 5'-TCCGTGATGTTAATGTGCTGG-3'
Pfk for5'-GGTCGCTTGAAAGCCGCTA-3'
Pfk rev 5'-CTGACGGAACAGATTGGCG-3'
Pyk for 5'-GCAGGAGCTGATACCCAACTG-3'
Pyk rev 5'-CGTGCGATCCGTGAGAGAA-3'

Climbing Assay

The climbing assay was performed as previously described (Iijima-Ando et al., 2009). Approximately 30 flies were placed in an empty plastic vial (2.5 cm in diameter x 8 cm in length). The vial was gently tapped to knock the flies to the bottom, and the height that the flies climbed in 30 seconds after tapping to the bottom of the vials was measured. Experiments were repeated more than three times, and a representative result was shown. Food vials were changed every 2-3 days.

Lifespan Analysis

Food vials containing approximately 25 flies were placed on their sides at 25°C under conditions of a 12 hour:12 hour light:dark cycle. Food vials were changed every 2-3 days, and the number of dead flies was counted each time. At least three vials for each genotype were prepared.

Calorie restriction

Flies were raised on the regular cornmeal described above. After eclosion, female flies were maintained on regular cornmeal food, food without cornmeal and containing 10% (w/v) of yeast and glucose (10%), or food without cornmeal and containing 1% (w/v) of yeast and glucose (1%). Flies were placed at 30 flies/vial, and food vials were changed every 2-3 days.

Glucose assay

Glucose assay (HK) was performed as previously described with mild modifications (Tennessen et al., 2014). Flies were frozen with liquid nitrogen and heads and bodies were isolated. 40 heads and 10 bodies were collected and homogenized in 100 μl PBS. The sample extract was centrifuged at 16,000 g at 4°C. The supernatant was heated at 70 °C for 10 min and centrifuged at 16,000 g for 3 min at 4°C. Glucose levels were measured using by HK reagent (Sigma). Protein levels were measured using by Bradford assay.

Immunohistochemistry and image acquisition

For adult brain dissections, females were collected 1-2 days after eclosion and maintained at 25 °C until the required age. Dissections were performed in PBS, and samples were fixed for 30min in formaldehyde (4% v/v in PBS) at room temperature and washed for 10 min with PBST containing 0.1% Triton X-100 three times. For blocking, samples were incubated for 1h at room temperature in 1% normal goat serum (Wako, Cat# 143-06561) in PBST and incubated overnight with the primary antibody, anti- Elav (1:50; Developmental Studies Hybridoma Bank, Cat# 9F8A9, RRID:AB_528217), diluted in 1% NGS/PBST at 4 °C. After the primary antibody, samples were washed for 10 min with PBST including 0.1% Triton X-100 three times and incubated with the secondary antibody for 3 hours at room temperature. Samples were mounted in Vectashield (Vectorlab Cat#H-1100) and captured images on a Keyence BZ-X700.

Statistics

The number of replicates, what n represents, precision measurements, and the meaning of error bars are indicated in Figure Legends. Data are shown as mean ± SEM. For pairwise comparisons, Student's t-test was performed with Microsoft Excel (Microsoft). For multiple comparisons, data were analyzed using one-way ANOVA with Tukey's HSD multiple-comparisons test in the GraphPad Prism 6.0 software (GraphPad Software, Inc., La Jolla, CA). For survival analysis, p-value by log-rank test compares the entire curve in the GraphPad Prism 6.0 software. All results were considered statistically significant a p-value of less than 0.05 was considered to be statistically significant.

Supplemental references

Besson, M.T., Alegria, K., Garrido-Gerter, P., Barros, L.F., and Lievens, J.C. (2015). Enhanced neuronal glucose transporter expression reveals metabolic choice in a HD Drosophila model. PLoS One 10, e0118765.
Iijima-Ando, K., Hearn, S.A., Shenton, C., Gatt, A., Zhao, L., and Iijima, K. (2009). Mitochondrial mislocalization underlies Abeta42-induced neuronal dysfunction in a Drosophila model of Alzheimer's disease. PLoS One 4, e8310.
Imamura, H., Nhat, K.P., Togawa, H., Saito, K., Iino, R., Kato-Yamada, Y., Nagai, T., and Noji, H. (2009). Visualization of ATP levels inside single living cells with fluorescence resonance energy transfer-based genetically encoded indicators. Proc Natl Acad Sci U S A 106, 15651-15656.
Livak, K.J., and Schmittgen, T.D. (2001). Analysis of relative gene expression data using real-time quantitative PCR and the 2(-Delta Delta C(T)) Method. Methods 25, 402-408.
Perkins, L.A., Holderbaum, L., Tao, R., Hu, Y., Sopko, R., McCall, K., Yang-Zhou, D., Flockhart, I., Binari, R., Shim, H.S., et al. (2015). The Transgenic RNAi Project at Harvard Medical School: Resources and Validation. Genetics 201, 843-852.
Tennessen, J.M., Barry, W.E., Cox, J., and Thummel, C.S. (2014). Methods for studying metabolism in Drosophila. Methods 68, 105-115.
Tsuyama, T., Kishikawa, J., Han, Y.W., Harada, Y., Tsubouchi, A., Noji, H., Kakizuka, A., Yokoyama, K., Uemura, T., and Imamura, H. (2013). In vivo fluorescent adenosine 5'-triphosphate (ATP) imaging of Drosophila melanogaster and Caenorhabditis elegans by using a genetically encoded fluorescent ATP biosensor optimized for low temperatures. Anal Chem 85, 7889-7896.